P2.1 ON THE ROLE OF THE ROCKY MOUNTAINS IN FORCING LOW-LEVEL JET IN THE CENTRAL U.S

Zaitao Pan*, Moti Segal and Raymond W. Arritt
Department of Agronomy, Iowa State University, Ames, IA 50011

1. INTRODUCTION

The present consensus is that the most important forcing mechanisms for the low-level jet (LLJ) are the response to diurnal boundary-layer evolution over slopes and the dynamical relationship to upper-level flow. It has to be emphasized that these two types of processes must not be viewed as competing or mutually exclusive explanations for the LLJ. Rather, the characteristics of the LLJ are established by their *combined* influences. General discussions of the combined forcing mechanisms have been given by Mitchell et al. (1995), Zhong et al. (1996), among others.

Although both theory and observation have extensively documented the Rocky Mountain slope effects on the LLJ, direct quantification of the contribution of the elevated terrain to the LLJ forcing, through elimination or modification of the topography in model simulations, has not been reported to our knowledge. A hypothetical modification of the topography in the continental U.S. in a model simulation will affect the characteristics of the LLJ which are topographically forced. Adopting such an approach would provide complementary insight into the knowledge obtained in previous LLJ studies. Particularly it would outline a reference meteorological state absent of the topographical forced processes. Alteration of the topography in model simulation is likely to modify the following simulated LLJ related forcing: (i) the background southerly flow in the south-central U.S., which prevails during summer as a result of modification of the summer meteorological systems over the region, in particular the continental ridging form the Bermuda High. Also it would modify lee-side cyclogenesis in the eastern slopes of the Rocky Mountains. (ii) the along-slope induced nocturnal thermal gradient and the related mesoscale ageostrophic flow component that contributes to LLJ formation.

Modifying the topography in a model simulation will allow the combined effects of (i) and (ii) above to be examined. Such simulations are likely to provide also some insight into the relative role of the topography in contribution to individual processes that forces the LLJ in the central and southern U.S. In this Note we selected the 1993 summer flood period in the central U.S. in which LLJs were frequent and intense. In sensitivity simulations we reduced the topography in the domain and examined the impact on the climatological patterns of the meteorological systems and the LLJ related characteristics and forcings. Evaluations are made in terms of time-averaged properties during the simulation period.

*Corresponding author address: Zaitao Pan, 3010 Agronomy Hall, Iowa State University, Ames, IA 50011; e-mail: panz@iastate.edu

2. METEOROLOGICAL CONDITIONS AND METHODOLOGY OF EVALUATION

2.1 Numerical modeling approach

Regional climate model forced continuously in time by observed meteorological lateral boundary conditions would likely maintain the large-scale atmospheric conditions of 1993 in the modified topography simulations. If lateral boundaries are not too close or too far from the center of the domain this approach would provide a reasonable compromise for the modeling evaluation.

The NCAR/Penn State mesoscale model MM5 is used in this study. The OSU land surface model (Chen and Dudhia 2001) was adopted. The lateral boundary conditions were imposed by considering an 11 grid-point nudging zone adjacent to each lateral boundary where the weighting of the observations was reduced linearly away from the boundaries to the interior of the model domain. The initial and lateral boundary conditions were derived from the NCEP/NCAR reanalysis (Kalnay et al. 1996) and updated every 6 hours.

2.2 Experiment setting

We performed a 45-day continuous model integration forced by lateral boundary conditions using the NCEP/NCAR reanalysis. The simulated period was 1 June – 15 July 1993, the peak LLJ active period. The full terrain experiment (CTRL) uses the actual topography as resolved by the model 52 km grid. The highest terrain elevation of 3140 m resolved by the model is a gross measure for topography. The second experiment is flat terrain (FLAT) where the terrain heights are set to zero.

3. RESULTS

3.1 Averaged geopotential heights and flow

In this sub-section we present simulated 45-day averaged lower atmosphere geopotential heights and flow patterns implying potential LLJ characteristics. It would be difficult to present the average flow during LLJ

events for the simulated period, because of the spatial and temporal variation of the LLJ from one case to another. Therefore we present the simulated 45-day averaged geopotential and flow, which imply the potential for LLJ development.

The geopotential height is presented at 850 hPa (Fig. 1a), which corresponds approximately to the elevation where LLJ peak intensity is commonly observed in the High Plains. Note that in CTRL, for locations where the topography is greater than ~1500 m the geopotential height was extrapolated to 850 hPa. Simulated geopotential fields obtained at a higher level (700 hPa) in CTRL and in a simulation where 0.5 of actual terrain height was considered (not shown) implied corresponding realistic features of the 850 hPa geopotential fields at these locations. In the CTRL simulation for 06 UTC (around local midnight) a well defined ridging from the Bermuda High is simulated east of the Rocky Mountains accompanied by a troughing at the lee-side, in agreement with the observed pattern reported in Arritt et al. (1997). The corresponding flow is presented at the level σ=.91 (~700 m above the surface; reflecting typical height of LLJ maximum). Intense flow is most pronounced in western Texas, Oklahoma and Kansas with a maximum ~16 m s^{-1} (Fig. 1a). The core of the strong flow extended eastward into Missouri. In FLAT, lack of topographical blocking resulted in a significant westward expansion of the ridge from the Bermuda High, while the lee-side troughing was eliminated (Fig. 1b). Orientation of the geopotential contours turned more zonal, while the geopotential gradient over the central U.S. was weakened, suggesting reduced geostrophic flow. In the absence of topography, a northward shift of the average tracks of synoptic systems crossing the U.S. is implied (in the CTRL simulation, on average the systems are deflected somewhat southward by the topography). In FLAT flow in the central U.S. is much less intense than shown previously in CTRL. The flow in northern Texas, Oklahoma, and Kansas weakened noticeably. However in the absence of mountain blocking noticeable penetration and strengthening of the easterly flow from the Gulf of Mexico in eastern Mexico is evident.

The 45-d average difference in wind velocity (CTRL minus FLAT) at σ=0.91 at 06 UTC showed a pronounced cyclonic flow perturbation centered over the western U.S. (not shown) This perturbation is suggested to be forced by the combined effects of topographical flow blocking, lee-side cyclogenesis and thermally induced low pressure perturbation over the elevated terrain in the control simulation. The southerly flow component difference was enhanced east of the Rocky Mountains. The stronger daytime southerly flows in CTRL facilitate conditions conducive to the formation of nocturnal LLJ in the south-central U.S.

3.2. Low-level jet frequency

The LLJ frequency during the simulated period was computed according to Bonner's (1968) classification which is based on the vertical wind shear and maximum wind speed. Figure 2 presents the frequency of LLJ occurrence for Bonner's classes 2 and 3 (excluding the weaker LLJ class 1), corresponding to 16 and 20 m s^{-1} of peak wind speed, respectively. Bonner's class 1 was not considered since the model simulated winds were somewhat overpredicted. The LLJ frequency in CTRL at 06 UTC east of the Rocky Mountains was confined to a wide swath extending from northern Mexico to Iowa (Fig. 2a). The LLJ frequency had a primary peak at the U.S.-Mexico border in southern Texas (60%) and a secondary peak at Oklahoma (45%). The FLAT simulation has lower LLJ frequency in this region (Fig 2b). Thus the various topographic forcings in CTRL should explain most of the occurrence of LLJs. Although our focus is on the LLJ east of the Rocky Mountains it is worth pointing out that the simulated LLJ frequency peak over Montana in FLAT. The peak is explained by the lack of topographical southward deflection effect on the eastward moving cyclonic system, which resulted in a northward shift of tracks for these systems. Shallow baroclinic systems likely induced the LLJ in this location. However, it should be noted that the occurrence of the peak in the vicinity of the domain's lateral boundary may distorted its feature.

3.3 Vertical structure of wind and potential temperature

Evaluating the topographical impact on the LLJ, we present also east-west vertical cross-sections (its location is indicated in Fig. 1a) of the 45-d averaged potential temperature and wind speed for the CTRL and FLAT simulations at 06 UTC (Fig. 3a, b). The vertical cross-section passes through the location of the peak LLJ frequency in Oklahoma simulated in CTRL. The CTRL shows a well-defined LLJ structure (i.e., local wind maximum) over the slopes with wind speed maximum of ~16 m s^{-1}. However, in FLAT there was no evidence of LLJ vertical structure, and the peak wind only reached about 5 m s^{-1}. Comparing Figs. 3a and 3b it is evident that east of the Rocky Mountains in the average the LLJ is associated strongly with the along-slope nocturnal thermal gradient, in agreement with McNider and Pielke (1981). However, while in McNider and Pielke (1981) 2-D simulations the background flow was southerly, thus the slope thermal gradient was forced solely by the nocturnal diabatic cooling, in the present simulation the gradient was additionally supported by the nocturnal westerly advection of warm air from the elevated terrain. In locations where horizontal potential temperature gradients are mild or absent there is no vertical structure of LLJ (see Figs. 3a,b). Thus it appears that the slope induced thermal gradient contributes significantly to the formation of a pronounced LLJ. The decay of nocturnal boundary-layer turbulence, though conducive to intensification of the flow, is insufficient by itself to establish in the average the LLJ, as evident from examining FLAT (Fig. 3b). Also it may be suggested that in CTRL when an easterly flow component exists on the slopes following sunset, the development of nocturnal temperature inversion increases the Froude number and furthermore enhances topographical blocking of the flow.

4. CONCLUSIONS

In this study we presented sensitivity simulations that explored simulated changes in the LLJ, in which terrain elevation was reduced. Such an approach has not been reported, and it provides complementary insight to previous studies of LLJ. The integration period is a 45-d window selected from the 1993 flood when strong LLJs were frequent. Evaluations were made in terms of time-averaged properties during the simulation period.

Simulations with different terrain heights enabled quantification of the profound impacts that the Rocky Mountains have on LLJ strength, frequency and location through flow blocking, lee-side cyclogenesis, and along-slope induced nocturnal thermal gradient. Particularly the results illustrated the impacts of topographical blocking on constraining the westward expansion of the Bermuda High. Also illustrated quantitatively is the intensification of the southerly flow east of the Rocky Mountains due to topographical blocking. The potential vorticity theory explains the formation of the lee-side cyclogenesis for the westerly flow, an anticyclonic system for the easterly flow interacting with the Rocky Mountains. However, quantification of these features in the real world require sensitivity simulations as these carried out in the present study. In sensitivity simulations to terrain height modifications, it was found that the potential topography effects on LLJ intensity and frequency declined for low terrain.

ACKNOWLEDGEMENTS

The study was supported by NSF grant ATM-9911417, the Iowa State University Agronomy Endowment Funds and the Biological and Environmental Research Program (BER), U.S. Department of Energy, through the Great Plains Regional Center of National Institute for Global Environmental Change (NIGEC) under Cooperative Agreement No. DE-FC03-90ER61010). Computer resources used for this study were provided by NCAR CSL facility.

REFERENCES

Arritt, R.W. T.D Rink, M. Segal, D.P Todey, C.A. Clark., M.J. Mitchell., and K.M. Labas, 1997: The Great Plains low-level jet during the warm season of 1993. *Mon. Wea. Rev*., **125**, 2176-2192.

Bonner, W.D., 1968: Climatology of the low-level jet. *Mon. Wea. Rev.*, **96**, 833-850.

Chen, F., and Dudhia, 2001: Coupling an advanced land surface-hydrology model with the Penn State-NCAR MM5 modeling system. Part I: model implementation*. Mon. Wea. Rev*., **129**, 569-585.

Kalany, E. M, and co-authors, 1996: The NCEP/NCAR 40 years reanalysis project. *Bull. Amer. Meteor. Soc.,* **77**, 437-471.

McNider, R. T. and R. A. Pielke, 1981: Diurnal boundary-layer development over sloping terrain. *J. Atmos. Sci.*, **38**, 2198-2212.

Mitchell, M. J., R. W. Arritt, and K. Labas, 1995: A climatology of the warm season Great Plains low-level jet using wind profiler observations. *Wea. Fore.*, **10**, 576-591.

Zhong, S., J. Fast and X. Bian, 1996: A case study of the Great Plains low-level jet using wind profiler network data and high resolution mesoscale model. *Mon. Wea. Rev.*, **124**, 785-806.

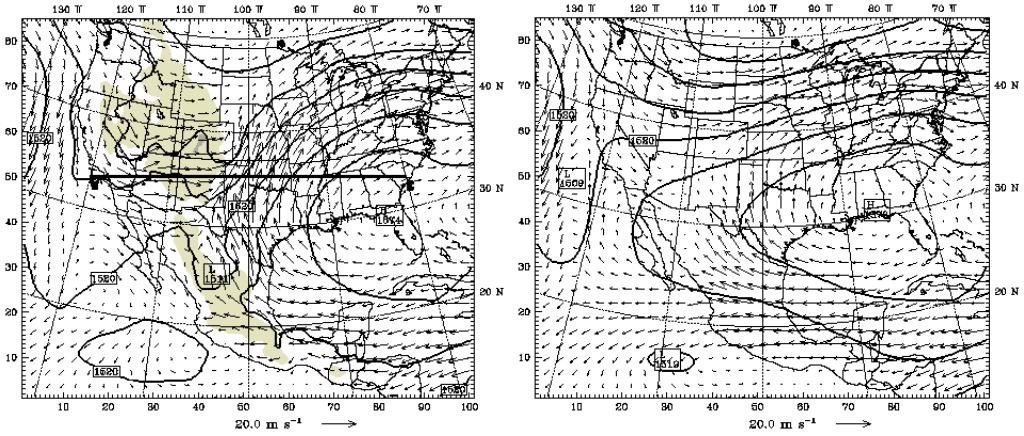

Fig. 1. Simulated 45-d averaged geopotential height at 850 hPa and wind velocity at σ=.91 (~700 m AGL): (a) CTRL and (b) FLAT at 06 UTC. Shading indicates terrain elevation higher than 1500 m.

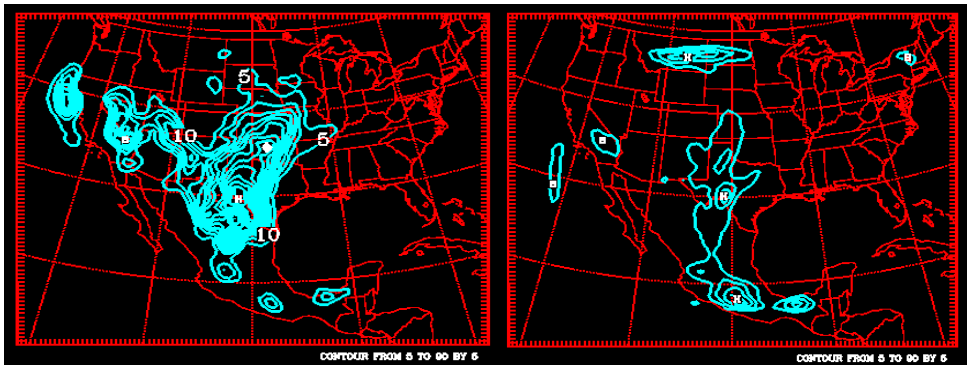

Fig. 2. Low-level jet frequency (%) for Bonner's classes 2 and 3 at 06 UTC for the simulated 45-d period: (a) CTRL and (b) FLAT. The ♦ indicates location of peak frequency.

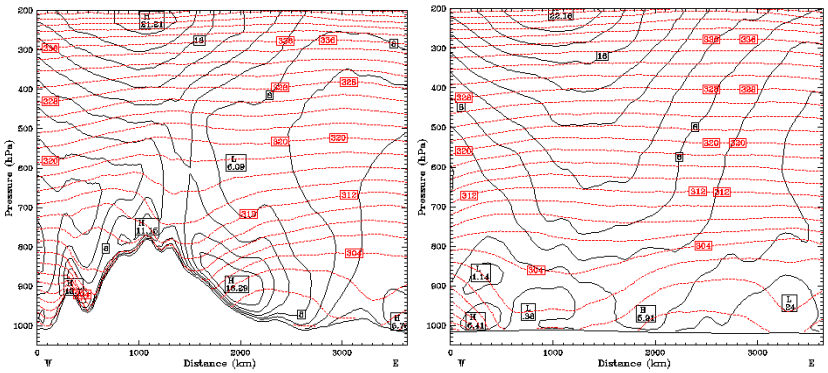

Fig. 3. Vertical cross-section of the 45-d averaged wind speed (solid contours) and potential temperature (dashed contours) along the dark line (E-W) marked in Fig. 1a at 06 UTC: (a) CTRL and (b) FLAT.